Università degli Studi di di Milano

FACOLTÀ DI SCIENZE E TECNOLOGIE
Corso di Laurea Triennale in Fisica

Turbulence Driven Clustering in Nematic Active Particles

Candidato:
Devin Waas
Matricola 793536

Relatori:
Dr. Marco G. Mazza (Esterno)
Prof. Alberto Vailati

Anno Accademico 2014-2015

Contents

Chapter 1

Motivation

The title of the work seems such a technical and specific subject. Hopefully, after reading this chapter the reader will be able to appreciate how clustering can be important in systems where nematic active particles are swimming in low Reynolds fluids.

Active Particles are basically anything that can move by means of self propulsion: bacteria are active particles; animals, including humans, are active particles; even cars and planes can be seen as active particles. In biological systems, usually the term is used to describe particles that propel themselves using ATP (adenosine triphosphate), the biological energy currency used in the cellular metabolism, to engage any kind of structure mainly made of proteins such as muscles or flagella. When the ATP is broken down into ADP + P the muscle or flagella contract, and movement is possible. There are several different types of active particles[1]. Among active particles, swimmers are the most studied since they are a simple and very general way to describe particles interacting with a fluid. Swimmers are insects, birds, fishes or bacteria. In our case, the last category is the one we are most interested in. Swimmers move in a different variety of ways and are classified mainly according do their moving mechanisms:
We have pullers which tend to use their flagella or cilia (or whatever organ) to pull the weight of the particle forward (think of someone who is climbing a mountain).
We have then pushers which do the opposite; they use their organs to push themselves forward. This category is the one closer to our personal experience because fishes usually are pushers and birds are too. We are interested in studying a specific type of pushers: the ones that adapted to move in fluids where viscosity prevails on inertia, that is, fluids with low Reynolds numbers. In particular, we want to study bacteria that move through a run and tumble mechanism. The preferred example we will often use in this work is one of the most studied model microorganism: the *Escherichia coli* (E. coli).

Nematic Particles were initially intended as, very inanimate liquid crystals. Liquid crystals are rod-like molecules that are widely used in everyday technology (e.g. LCDs, that is, Liquid Crystal Displays). The elongated shape of these molecules gives them anisotropic interaction, that is, the potential energy

between two such molecules depends on the mutual orientation and not just the distance between the centres of mass. Macroscopically, these substances exhibit thermodynamic phases intermediate between the liquid and crystalline symmetry, hence their name. As the temperature decreases, the system goes through a first symmetry breaking; there is a transition from an isotropic state, where molecular orientations are all disordered, to a state where one global, average orientation for the liquid crystals emerges. This is called the nematic director and the phase nematic. Importantly, molecules have head-tail symmetry, that is, the interaction is invariant upon transformation $\vec{u}_i \to -\vec{u}_i$, where $\vec{u}_i$ is the unit vector that describes the orientation of particle i. Upon further cooling other symmetry breaking occurs, for example, in the smectic phase there is a one dimensional ordering of the molecular centres of mass. The molecules forms layers. Within these two dimensional layers the system is still liquid, however, in the third dimension it is solid-like. It turns out that not only liquid crystals behave this way, many living creatures possess similar interactions and similar phase transitions[2]. For this reason, in last few decades, nematic models have been widely applied in the study of:

- bacteria(E. Coli)
- algae(Chlamydomonas[1])
- human cells (Granulocytes[3], Fibroblasts[4], Osteoblasts[4], Adipocytes[4], Melanocytes[4]).

And even though the shape of these particles seems far from isotropic, our work will show that under a given set of conditions isotropic behaviour can be found in clusters.

Turbulence is a delicate matter. We know that the majority of the phenomena in nature are turbulent, but we know really little about turbulence itself. Examples of turbulence can be extreme, like a whirlpool; or more subtle, like the smoke rising from a cigarette. Even the blood in our vessels is a good example of turbulent fluid flow. Very useful results have been found when studying birds[5], fishes[6], and locusts[7] as active particles in turbulent environment.

We will focus on micro-scale organisms. Usually when a microorganism swims in a viscous fluid, it generates a flow that interacts with the near particles[8]. In the case of high density of particles, the phenomena can even originate spectacular sights such as bacterial turbulence. Bacterial turbulence is a good example of a large scale turbulent phenomenon generated by the mutual interaction between bacteria. In this case, it is possible to observe large scale of intermittent swirls and jets that manifest themselves once a certain concentration of swimmers is reached[9, 10, 11, 12, 13, 14, 15, 16].

Examples of such high densities need not to be sought very far for they can be found even in humans. Think of the millions of spermatozoa that swim towards egg cells for fertilisation[17].

Clustering is a way to say that many particles occupy a very little volume. Clusters can have very different collective properties from the ones the single particles that compose them possess. In nature, clustering is a phenomenon that becomes extremely relevant in the case of a small number of particles,

especially in the case of reproduction. The wood mouse spermatozoa, for example, are individually able to swim faster when in a clustered state[18], opossum spermatozoa pair themselves so that they can swim more efficiently in very viscous fluids[19] and fishfly spermatozoa cluster in dense bundles to gain similar advantages[20].

Our work focuses on systems populated by nematic active particles that move with a run and tumble mechanism. The particles we model move at a constant speed (they move in a low Reynolds fluid). We study the clustering of these particles and show that the turbulence strongly facilitates aggregated states. For clustering purposes, the turbulence helps the particles reduce the effects of thermal noise, this suggests that the adjusting of the inter-particle interaction could be an effective mechanism used by the organisms to cluster themselves and gain biological advantage.
The reason we are so excited about this research is that the majority of theoretical and numerical investigation in the world of liquid crystals were done in two or quasi-two dimensional settings. Thanks to the efficient code and the machines available at the Max Planck Institut Für Dynamik und Selbstorganisation, it is now possible to explore new computational frontiers.

Chapter 2

Introduction

This chapter focuses on introducing the reader to the field of research of our work. The first section offers a very quick comparison and an explanation on where our model fits in the current research paradigm; the second section is a quick recap of the important notions of turbulent fluid mechanics; the third and last section goes deep into the theoretical details of our model; the implementation details are left to the next chapter.

2.1 Previous Systems

Since Vicsek proposed a model for bird flocking, in 1995[5], the field of study of the active particles has been full of discoveries. In 2013, Stocker et al. [21] published a paper called "Turbulence drives microscale patches of motile phytoplankton" a study that shows how turbulence facilitates clustering of spherical active particles; this prompted us to study the clustering of the nematic particle counterparts. Follows a quick comparison of the models that are similar to the one used in this work.

Stocker's System studies spherical particles that are affected by gravity (heavy bottomed). Particles are interacting with one another only through the turbulent field which, as we remind, is generated by the mutual interaction of the particles. Turbulence is calculated solving the Navier-Stokes equations with the finite element software COMSOL Multiphysics. The main results are that the active particles cluster, but dead cells do not. This also suggests that the particles need to be active to cluster in a turbulence driven manner.

The Mazza-Breier System is the model that was used as a starting point for our model. The particles are nematic and swim at a constant speed (low Reynolds numbers). The particle-particle interaction is given by the Lebwohl-Lasher potential (later defined) and there is no direct turbulence involved.

Our Model implements the same Lebwohl-Lasher potential of the Mazza-Breier model to calculate the geometrical interactions of the particles and uses the turbulence to model the interactions that are of a hydrodynamic type. The equations of motion we used in the molecular dynamics simulations can be found

in last section of this chapter. A few examples of how our implementation helps us achieve uncommon speed are given by the Kraichnan method, used instead of solving Navier Stokes equations, and the use of a Monotonic Logic Grid to quickly calculate neighbour interactions. Implementation details will be covered in the next section.

2.2 Fluid Mechanics

A full treatise on turbulent fluid dynamics is far from the aim of this section. This section introduces only the main physical quantities that are relevant for our work and is adapted from Kundu's "Fluid Mechanics" [22].

2.2.1 Some Definitions

First of all, it is important to introduce some concepts of general fluid dynamics; they are required to understand the turbulence in the system. It is however important to say that our model does not simulate directly the fluid; the hypotheses we make on the fluid only affect the interactions between particles. For what pertains our model, the turbulent flow we look at is incompressible, stationary, homogeneous, isotropic and normal multivariate.

Incompressible Flow A flow is called incompressible if the fluid does not change it's density in response to pressure changes. That is, the material derivative of the density is equal to zero. Equation (2.1) shows the infamous continuity equation in three dimensions; a property that directly descends from the continuity equation is that incompressible flows are also divergent-less, that is, $\vec{\nabla} \cdot \vec{u} = 0$.

$$\frac{d\rho(\vec{x},t)}{dt} + \vec{\nabla} \cdot (\rho(\vec{x},t)\vec{u}(\vec{x},t)) = 0 \tag{2.1}$$

where $\rho(\vec{x},t)$ as the density of the fluid, in a point in $\vec{x}$ in space and at a given time t; and $\vec{u}$ is the velocity field evaluated in the same conditions as ρ.

In physics, incompressibility is a very common hypothesis, in fact, liquids are almost always incompressible and so are gasses with flow velocities less than ~ 100 $\frac{m}{s}$ (or less than $Mach$ 0.3). This definition is so important for us because, in the Kraichnan method we use to compute turbulent velocity fields, incompressibility of the fluid is an hypothesis. Constant density flows, a subset of incompressible flows, can also have their Navier-Stokes equations conveniently rewritten in a way that gravity can be ignored (more of this can be found at page 135 of the Kundu).

Navier-Stokes Momentum Equation The Navier-Stokes equations have the role of Newton's equations in fluid mechanics; they are however highly non-linear and this is the main reason for which solving Navier-Stokes equation is so difficult and it is why, for three dimensional models, we have no analytical solution yet.

Equation (2.2) shows the Navier-Stokes system of differential equations for an incompressible flow.

$$\rho \frac{D\vec{u}}{Dt} = (+\rho\vec{g} - \nabla p) + \mu\nabla^2\vec{u} \tag{2.2}$$

where ρ is the fluid density; $\frac{D}{Dt}$ is the total derivative defined as $\frac{DF}{Dt} = \frac{dF}{dt} + \vec{u} \cdot \vec{\nabla}F$; $\vec{p}$ is the pressure; $\vec{g}$ is the gravitational acceleration; μ is the viscosity of the fluid.

The term at the left hand side of the equation is the total derivative of the velocity field (times a density): the first term is simply the variation in time, the second term is more interesting because it has the form of $\vec{u} \cdot \vec{\nabla}u$; it is the advective flow term of the velocity field and it represents the changes that the velocity has when the particles of the fluid move in space. Let's look at the right hand side: the first two terms are the internal (pressure) and external (gravity) forces acting on the fluid, the third term is the viscous term and represents the diffusion of the velocity.

Our Equations of Motion In our model, gravity will be neglected, so the first term of the right hand side of the equation will be ignored.

In our equations of motion we will also exploit the fact that an incompressible flow's laplacian can be written as it's curl (see equation (2.3)).

$$(\mu\nabla^2\vec{u})_j = -\mu(\vec{\nabla} \times \vec{\omega})_j \tag{2.3}$$

where j is the selected component; and $\vec{\omega}$ is the vorticity of the flow defined as ($\vec{\omega} = \vec{\nabla} \times \vec{v}_{turb}$).

Dynamics of the Fluid The reason the Navier-Stokes momentum equations (2.2) and the continuity equation (2.1) are so important in fluid mechanics is that, if combined with suitable boundary conditions, these 4 equations with 5 variables (ρ, P, and u_j with $j = 1, 2, 3$) are able to completely describe the dynamics of our fluid.

Reynolds Number is a dimensionless number that helps to predict similar flow situations in different flow conditions.
Low Reynolds numbers are associated with laminar flow: a flow where viscous forces are dominant and the motion of the fluid is constant and smooth.
High Reynolds numbers are associated with turbulent flows: flows dominated by inertial forces that produce chaotic eddies, vortices and other flow instabilities.

$$\mathrm{Re} = \frac{\text{inertial forces}}{\text{viscous forces}} = \frac{\rho \vec{u} L}{\mu} = \frac{\vec{u} L}{\nu} \tag{2.4}$$

where $\vec{u}$ is the mean velocity of the object relative to the fluid; L is the characteristic length of the system; μ is the dynamic viscosity of the fluid; ν is the kinematic viscosity $\nu = \frac{\mu}{\rho}$; and ρ is the density of the fluid.

Scaling Often in fluid mechanics we encounter dimensionless parameters such as the Reynolds, the Richardson, or the Froude numbers (and many more can be defined). In turbulence, the Reynolds number helps us recognise classes of similar problems, that is, given a geometry for the problem (boundary conditions), if the number is lower than a critical value, we expect a laminar flow, else we expect to observe turbulence. The full power of describing the system with dimensionless numbers can be appreciated when the Navier-Stokes equation is cast to its dimensionless form. As we recall, with the continuity equation and the boundary conditions, we can completely describe the dynamics of the fluid in our system; in the dimensionless case, however we can also describe a whole class of dynamically similar systems, that is, systems that have the same dimensionless parameters and a scale-similar geometry; we only need to map the first flow into the second by multiplication of a single scale ratio. More information about this can be found at pages $143 - 150$ of the Kundu[22].

$$\frac{D\vec{u}'}{Dt'} = -\nabla' p' + \frac{\mu}{\rho L \overline{\vec{u}'}} \nabla'^2 \vec{u}' + \vec{g}' \tag{2.5}$$

where $\vec{u'} = \frac{\vec{u}}{\overline{\vec{u}}}$; $\vec{p}' = p \frac{1}{\rho \overline{\vec{u}}^2}$; $g' = \vec{g} \frac{L}{\overline{\vec{u}}^2}$; $\frac{\partial}{\partial t'} = \frac{L}{\overline{\vec{u}}} \frac{\partial}{\partial t}$; $\nabla' = L\nabla$; L is the characteristic length of the problem; $\overline{\vec{u}}$ is the mean velocity relative to the fluid; ρ is the fluid density.

Equation (2.5) shows the adimensional casting of the Navier-Stokes equation for incompressible fluids. We notice that the coefficient of the viscous term (the second on the right hand side) is the inverse of the Reynolds number $\frac{1}{\mathrm{Re}} = \frac{\mu}{\rho L \overline{\vec{u}}}$.

2.2.2 Turbulence

Turbulence is a wide studied yet not fully understood subject. One of the most important physicists of the past century, Richard P. Feynman said that turbulence is "the most important unsolved problem of classical physics".

The aim of this subsection is to explain the main results of research in turbulent fluid mechanics through a chronological exposition and then to define the useful quantities for a theoretical understanding of this work.

History of Turbulence The first work on turbulence was done by Osborne Reynolds in 1883. Doing experiments with pipe flows, he showed that when the dimensionless number $\mathrm{Re} = \frac{uL}{\nu}$ exceeds a critical value the system becomes turbulent. Then, he found that he could use this number to classify systems that have similar types viscous flows. Reynolds also introduced the way of writing a turbulent flow in mean component plus a fluctuating value; to the day the decomposition is called Reynolds Decomposition and its use is still widespread. The next great contributor is G. I. Taylor. In his work in 1921 he introduced the idea of correlation function, he then went on to show how the turbulent diffusion a particle from a source point initially increases with time linearly, then for large times, it increases with the square root of the time, just like a random walk[23]. During 1935-1936, Taylor also introduced the concepts of homogeneous and isotropic turbulence and of a turbulence spectrum. In 1915, Taylor introduced the idea of mixing length, the length that a particle needs to travel before giving up all of its original momentum and behaving like the surrounding fluid[24] (the mixing length is conceptually similar to the mean free path in thermodynamics).
Usually the mixing length is credited to Ludwig Prandtl who, during the 1920s, together with his student Von Karman, developed semi empirical theories of turbulence of which the most important result is that the average turbulent velocity profile near a solid wall is logarithmic.
In 1922, the British meteorologist Lewis Richardson wrote the first book on numerical weather prediction. In the book it was proposed that the turbulent kinetic energy is transferred from large to small eddies, until dissipated by viscous flow[25]. This spectral cascade idea is central in the present understanding we have of turbulence. Richardson is also credited for the proposal of his four-third law. The law states that the effective diffusion coefficient of a patch of turbulence is proportional to $l^{\frac{4}{3}}$, where l is the length scale of the patch.
Later, Kolmogorov hypothesised that the statistics of small scale eddies are isotropic and depend only on the following two parameters: the kinematic viscosity, ν and the average rate of kinetic energy dissipation, $\bar{\epsilon}$. From dimensional arguments he derived that the smallest possible scale has the size of $\eta = (\frac{\nu^3}{\bar{\epsilon}})^{\frac{1}{4}}$[26]. He also proposed that at the scales between l and η there must exist an inertial subrange with eddies that only depend on the parameter $\bar{\epsilon}$. Thanks to this idea, in 1941[27], Kolmogorov and Obukhov independently found that the spectrum in the inertial subrange must be proportional to $\epsilon^{\frac{2}{3}} k^{-\frac{5}{3}}$ where k is the wave number associated with the length scale of the eddy. This poses one of the most important results in turbulence and agrees with experimental results found at high Reynolds numbers.

Definition Although elusive by nature, the definition of the turbulent flow displays the following characteristics:

1. Fluctuations: turbulence always exhibits fluctuations in velocity, pressure and temperature that tend to be irregular, chaotic and unpredictable.

2. Nonlinearity: turbulence is a solution for Navier-Stokes equations which are a non-linear set of differential equations.

3. Vorticity: eddies are the building blocks of a turbulent flow. We understand that as the Reynolds numbers increase, the eddies sizes increase as well.

4. Dissipation: eddies evolve into smaller-scaled versions of themselves in a non-linear way so that eventually the fluid viscosity dissipates the eddies altogether. Energy needs to be constantly supplied to sustain turbulence.

5. Diffusivity: fluctuations facilitate mixing of different species, momentums, or even heat.

A simple, although imperfect, definition of turbulence is: "a dissipative flow state characterised by non-linear fluctuating three dimensional vorticity".

Turbulence Energy Cascade Studying where the energy goes can often bring insights on the phenomena; turbulence is no different: we will show that thanks to the Reynolds decomposition, it is possible to write two sets of equations for the kinetic energy. One for the mean flow and one for the turbulent velocity fluctuations. Thanks to the comparison of these two it will be easy to understand how the energy of our system is partitioned.

In turbulence, due to the fluctuating nature of the phenomenon it is useful to define quantities as following:

$$\tilde{u}_i = \overline{u}_i + u_i \tag{2.6}$$

$$\tilde{p} = \overline{p} + p \tag{2.7}$$

$$\tilde{\rho} = \overline{\rho} + \rho' \tag{2.8}$$

$$\tilde{T} = \overline{T} + T' \tag{2.9}$$

$\overline{u_i}$ is the mean velocity of the i-th component; u_i is the turbulent fluctuation; $\overline{p}$ is the mean pressure; p is turbulent fluctuation of pressure; $\overline{\rho}$ is the mean density; ρ' is turbulent fluctuation of density; $\overline{T}$ is the mean temperature; T' is turbulent fluctuation of temperature;

The mean quantities in equations (2.6),(2.7), (2.8), and (2.9) are regarded as expected values whereas the mean of the fluctuation is to be considered equal to zero.

This type of notation is called Reynolds decomposition and it is often used to write the Navier-Stokes equations in an averaged form, Reynolds averaging Navier-Stokes equations, for short, RANS equations.

We are interested in studying how the energy moves between the mean and the fluctuating kinetic energies. We can write an energy balance (or budget) equation for the mean flow:

$$\frac{\partial \overline{E}}{\partial t}+\overline{u}_j\frac{\partial \overline{E}}{\partial x_j}=\frac{\partial}{\partial x_j}(-\frac{\overline{u_j p}}{\rho_0}+2\nu\overline{u}_j\overline{S_{i,j}}-\overline{(u_i u_j)\overline{u_i}})-2\nu\overline{S_{i,j}S_{i,j}}+\overline{u_i u_j}\frac{\partial \overline{u_i}}{\partial x_j}-\frac{g}{\rho_0}\overline{\rho}u_3 \tag{2.10}$$

where $\overline{E}$ is the mean kinetic energy for the mean flow; $\overline{S_{i,j}}=\frac{1}{2}(\frac{\partial \overline{u_i}}{\partial x_j}-\frac{\partial \overline{u_j}}{\partial x_i})$ is the mean strain rate-tensor;

Let us see what each term of this equation means.
The left hand side of the equation shows the total derivative of the energy. The right side is where things become interesting.
The first three terms are called transport terms because they only move energy in space and do not generate or dissipate any. This can be seen by integrating the terms over the volume of our system and using the divergence theorem (Gauss theorem) to transform the volume integral into a surface integral; if $\overline{u_i}=0$ on the boundary the flux is zero. The first divergence term is the transport due to pressure, the second due to viscous stresses and the third is due to Reynolds stresses.
The fourth term at the right is the viscous dissipation term: it is the product between the mean flow's viscous stress and the mean strain rate. The fifth term is the shear production term, it represents the energy that the mean flow loses to the fluctuating velocity field. These two terms are tightly coupled, they represent the energy transferred between the two energy balance equations. These two terms are written with an opposite sign in the kinetic energy balance for the fluctuating velocity.
We will not spend too many words on the sixth and last term; it represents the work done by gravity but, as anticipated earlier, our system does not take in account gravity.

We can also write the balance equation for the fluctuating velocity field:

$$\frac{\partial \overline{e}}{\partial t}+\overline{u}_j\frac{\partial \overline{e}}{\partial x_j}=\frac{\partial}{\partial x_j}(-\frac{\overline{(u_j p)}}{\rho_0}+2\nu\overline{u_i S'_{i,j}}-\frac{1}{2}\overline{u_i^2 u_j})-2\nu\overline{S'_{i,j}S'_{i,j}}+\overline{u_i u_j}\frac{\partial \overline{u_i}}{\partial x_j}-g\alpha\overline{\vec{u}_3 T'}. \tag{2.11}$$

where $\overline{e}$ is the kinetic energy for the fluctuating velocity field; $S'_{i,j}=\frac{1}{2}(\frac{\partial u_i}{\partial x_j}-\frac{\partial u_j}{\partial x_i})$ is the mean strain rate-tensor;

In analogy with the other energy balance equation, the terms on the left hand side of the equation are the total derivative of the fluctuating kinetic energy and the first three terms on the right hand side are the transport terms.

The fourth term is the viscous dissipation of turbulent kinetic energy. At very high Reynolds numbers this term is not negligible as opposed to the analogous term found in the other energy balance equation; for this reason turbulence is a dissipative phenomenon.
The fifth term is the shear production term. As anticipated before, it represents

the energy that is gained from the mean flow.
The sixth term is the buoyant production (or destruction, if negative) term; it gives birth to interesting physics, but we won't discuss it because our system is not affected by gravity.

The shear production term is what drives the energy exchange between the mean flow and the fluctuating velocity field. For it to be active, the turbulence must be anisotropic. The system we study has isotropic turbulence, that is, the fluctuating energy balance reduces itself to equation (2.12) where only the transport terms survive.

$$\frac{\partial \overline{e}}{\partial t} + \overline{u}_j \frac{\partial \overline{e}}{\partial x_j} = \frac{\partial}{\partial x_j}(-\frac{\overline{(u_j p)}}{\rho_0} - \frac{1}{2}\overline{u_i^2 u_j}) \tag{2.12}$$

The same considerations apply to the mean flow equations 2.10.

2.3 Our System

This section describes the theory behind our model. The aim is set to show the mechanisms that affect the motion of the particles and to conclude the chapter with the starting point for molecular dynamics simulations: the equations of motion.

2.3.1 Our Active Particles

Particles come in a variety of sizes, and shapes. In the case of biological active particles these characteristics are not even required to be fixed: there can be genetic variance between members of the same species and, at the same time, the same particle could change its shape or speed. We are interested in modelling the collective behaviour of bacteria like the E. Coli, that is, nematic active particles that swim thanks to a run and tumble motion in low Reynold number fluids.

Run and Tumble As mentioned in the introduction, there are various types of swimmers. We can mainly distinguish them between pushers and pullers.

Birds and fishes need to deal constantly with fluids where inertial forces prevail, that is the reason why they adapted their motile organs this way.

Bacteria that populate viscous fluids need to use different propulsion mechanisms, that is how they evolved to have flagella that allow them to run and tumble.

The mechanism is simple: the particles initially propel themselves in a run phase, then they change orientation randomly in a tumble phase (see figure 2.1. The two steps are iterated continually. In this model, constant particle speed is used to recreate a low Reynolds fluid.

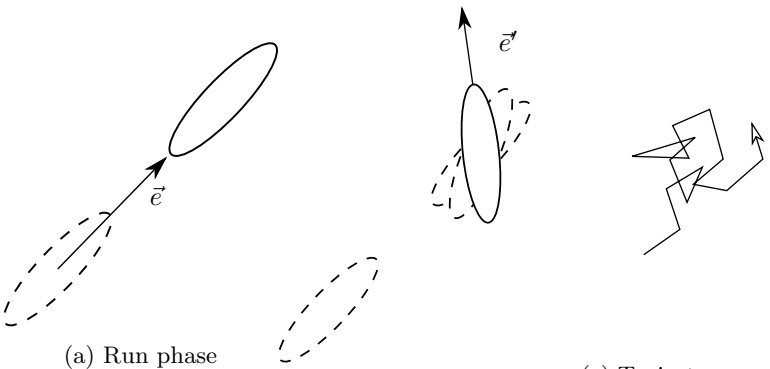

(a) Run phase

(b) tumble phase

(c) Trajectory example after a few cycles

Figure 2.1: Run and tumble motion

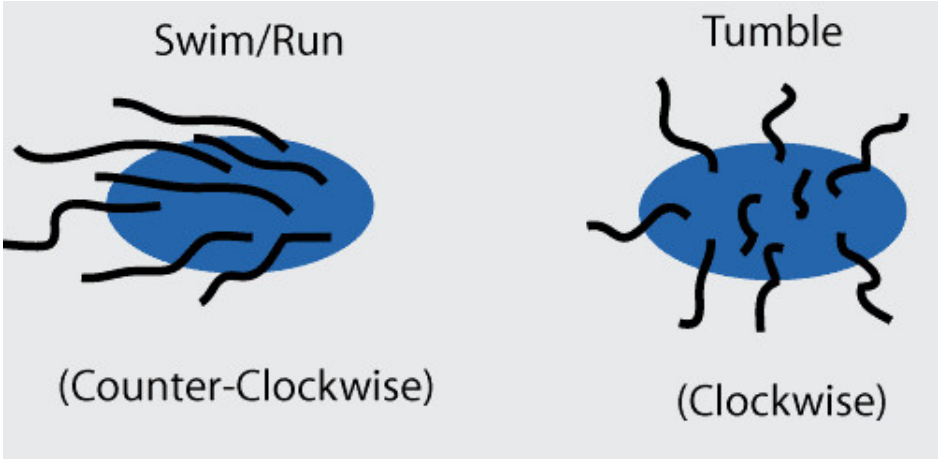

Figure 2.2: E. Coli run and tumble example

The E. Coli, for example has developed a very ingenious way of using its flagella: a counter-clockwise rotation causes the flagella to make the bacterium run, then a clockwise motion makes the bacterium tumble(see figure 2.2) .

Nematic Shape In the introduction, we saw that nature has quite a few examples where shape was selected for anisotropy. Nematic, or rod-like shapes are a perfect example of this type of natural selection. The shape is a very important characteristic of a particle because it affects the interaction between the environment (neighbours, boundraries), sets the ratio between volume and surface area, etc. Particles with this kind of elongated shape minimise their energy thanks to particle alignment rather than adjusting the distance between centres of mass. To model the nematic shape of the particles, we use an interaction potential called the Lebwohl-Lasher potential, defined as:

$$U = -\frac{1}{N_n}\sum_{j}^{N_n}(\vec{e}\cdot\vec{e}_j)^2 \tag{2.13}$$

where N_n is the number of neighbouring particles; $\vec{e}$ is the current particle direction; $\vec{e}_j$ are the neighbouring particles' directions.

Particles have head-tail symmetry, that is, the interaction is invariant upon transformation $\vec{u}_i \to -\vec{u}_i$, where $\vec{u}_i$ is the unit vector that describes the orientation of particle i.

Equation (2.13) reminds the Ising model's potential energy with one difference: the scalar product between the orientations is squared therefore energy will be minimised, as can be clearly seen in figure 2.3, by both parallel and anti-parallel alignments.

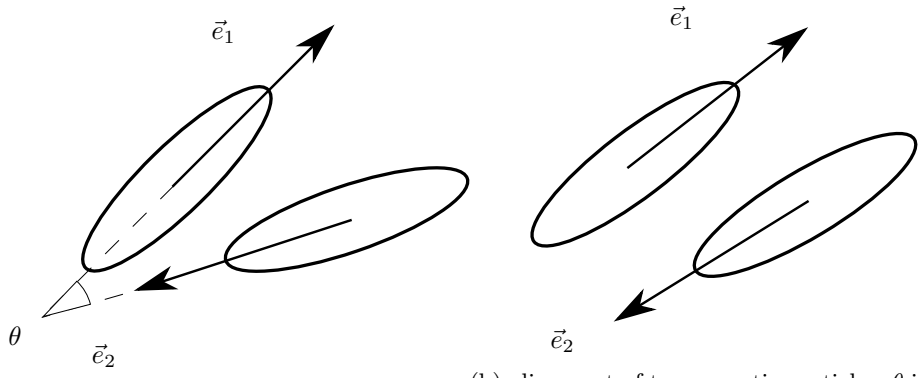

(a) Two nematic particles interacting

(b) alignment of two nematic particles; θ is minimised.

Figure 2.3: Nematic alignment

2.3.2 Nematic Order Parameter

Symmetries are a very powerful tool in physics. There are many examples where symmetries help us simplify the problem like for example in the case of the eigenvalue problem for the hydrogen atom. Other times, symmetries and general arguments help us understand the collectiv behaviour of the system. Liquid Crystals, for example, exhibit thermodynamic phases that are intermediate between the liquid and crystalline symmetry. As the temperature decreases, the system goes through a first symmetry breaking; there is a transition from an isotropic state, where molecular orientations are all disordered, to a state where one global, average orientation for the liquid crystals emerges. This is called the nematic director and the phase nematic. Upon further cooling, other symmetry breaking occurs, for example, in the smectic phase there is a one dimensional ordering of the molecular centres of mass. The molecules form layers. Within these two dimensional layers the system is still liquid, however, in the third dimension it is solid-like.

For each phase, there is an order parameter associated with it; a few examples are: nematic, smectic and ferromagnetic phases with the corresponding order parameters.

Our interest is to study how clustering affects the orientations of nematic particles, we will therefore focus on the nematic order parameter alone.

The nematic order parameter, also known as Maier-Saupe order parameter, is a quantity that describes the degree of alignment of the particles to an axis; the exact axis is unknown because the parameter is a scalar quantity. It is defined as the maximum eigenvalue of the following second order tensor:

$$S = \frac{1}{2N} \sum_{i=1}^{N} (3\hat{u}^i \hat{u}_i - \mathbb{I}) \tag{2.14}$$

where: N is the total number of particles in the system; $\hat{u}_i$ is the orientation of the ith particle; sum over the indices is implied (Einstein notation).

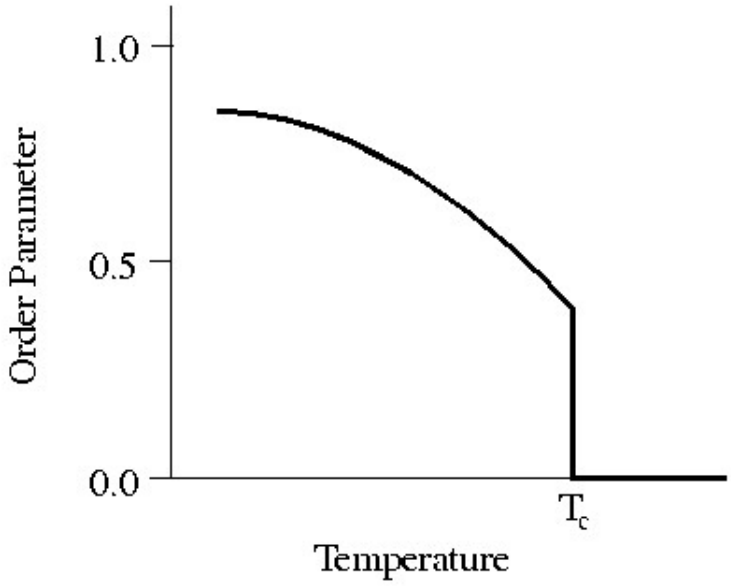

Figure 2.4: Nematic-Isotropic phase transition

Figure 2.4 shows a simple plot of the global nematic order parameter as a function of the temperature (in our system, the thermal noise η). The transition is continuous until a critical temperature is reached; there a symmetry breaking occurs and all the particles in the system become isotropically aligned.

$S = 0$ represents an isotropic system whereas a system with $S \simeq 1$ is a system that clearly has a preference in orientation.

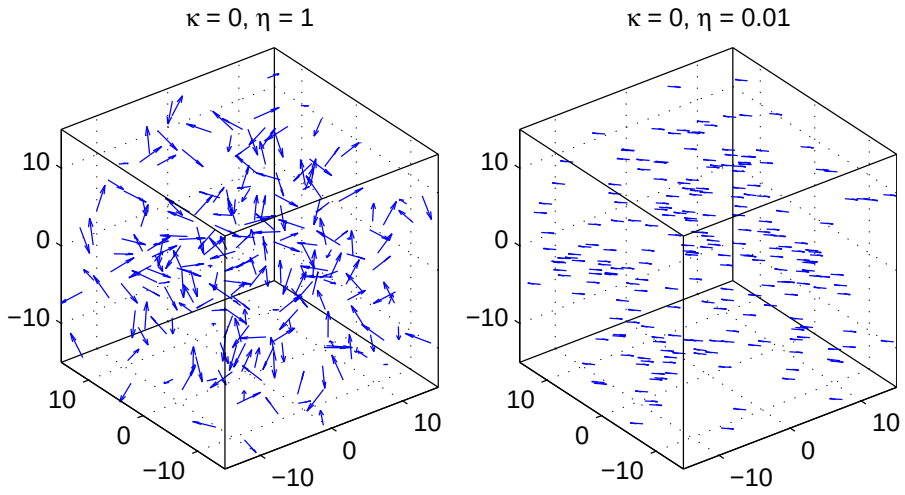

(a) Example of $S = 0$, isotropic system (b) Example of $S \simeq 1$, nematic system

Figure 2.5: Nematic and isotropic phases

Figure 2.5 shows the difference between an isotropic system and a homogeneous one. Both examples display the last snapshot of two simulations we ran where, for clarity, only 200 particles out of 27000 are randomly selected and printed. The arrows are printed at the particles positions and the arrows show the particle alignment; the length of the arrow is not proportional to the speed of the particles. In figure 2.5a it is easy to see that the arrows do not have any preferred direction, the system is therefore isotropic. In figure 2.5b the arrows all point from right to left or from left to right. They are therefore nematically aligned.

2.3.3 Clustering

As seen in the introductory chapter, clustering is an advantageous collective state that microorganisms like spermatozoa often exploit. Clusters can be characterised in many ways. Our main concern in this work is to distinguish and quantify clustered systems from homogeneous ones.

To measure the rate of clustering in the whole system, we define the patch enhancement factor Q[21] as

$$Q(f) = \frac{C(f) - C_{nm}(f)}{C_o} \tag{2.15}$$

where f is fraction of the particles with highest concentration; $C(f)$ is the mean concentration at a given f; $C_{nm}(f)$ is the mean concentration at a given f for the non-motile counterpart of our system; C_o is the mean concentration of the overall system, in our case this will always be $C_o = 1$.

This factor tells us that the f particles are Q times more concentrated than usual (e.g. $Q(0.1) = 12$ tells us that 10% of the particles are 12 times more concentrated than the density of the homogeneous system).

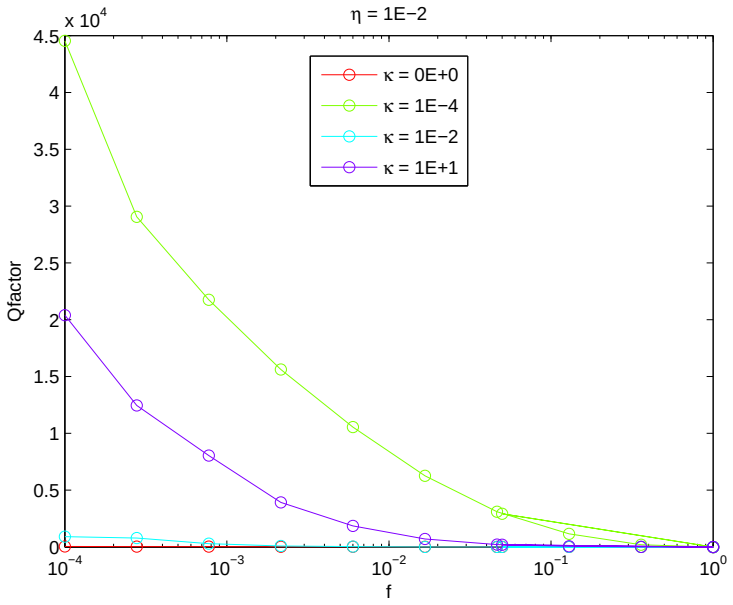

Figure 2.6: Q(f) plots; semilog axes

Figure 2.6 shows a few $Q(f)$ curves to give a gist of the behaviour of the function.
η is the thermal noise used defined in the Lebwohl-Lasher potential (see equation (2.13)); κ is the intensity of the turbulent field and will be defined more accurately in the explanation of Kraichnan's method. Thanks to figure 2.7 (it

shows the same curves with loglog axes), we can safely say that the curves approach zero and the fluctuations are due to floating point precision. Therefore our patch enhancement factor is well defined.

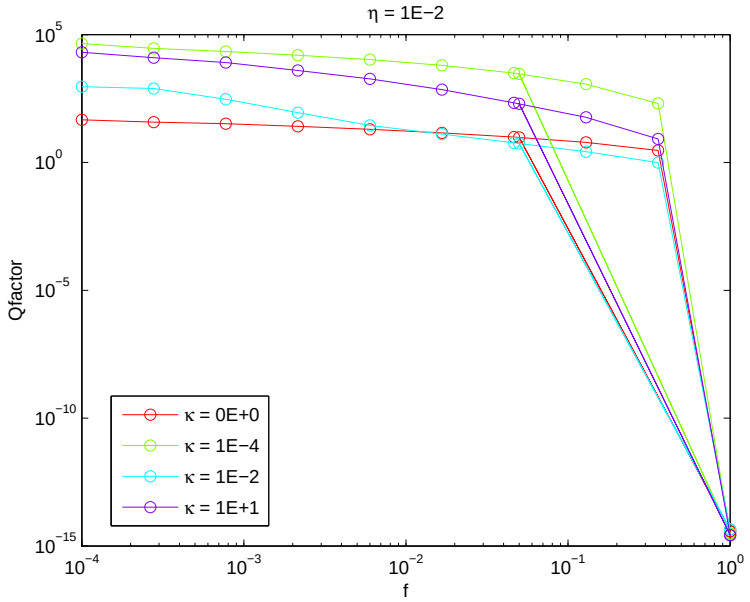

Figure 2.7: Q(f) plots; log log axes

Another way to characterise a cluster is to study its radius. We borrow from the study of molecules the common practice of using the radius of gyration.

The radius of gyration is defined in the following way:

$$R_g^2 = \frac{1}{N}\sum_{k=1}^{N}(\vec{r}_k - \vec{r}_{CM})^2 \tag{2.16}$$

where N is the number of total particles in the cluster; k is the index of the particles in the given cluster; $\vec{r_{CM}}$ is the mean position of the particles.

The gyradius is the root mean square of the particle positions in the cluster. It's a scalar quantity and it is always non-negative.

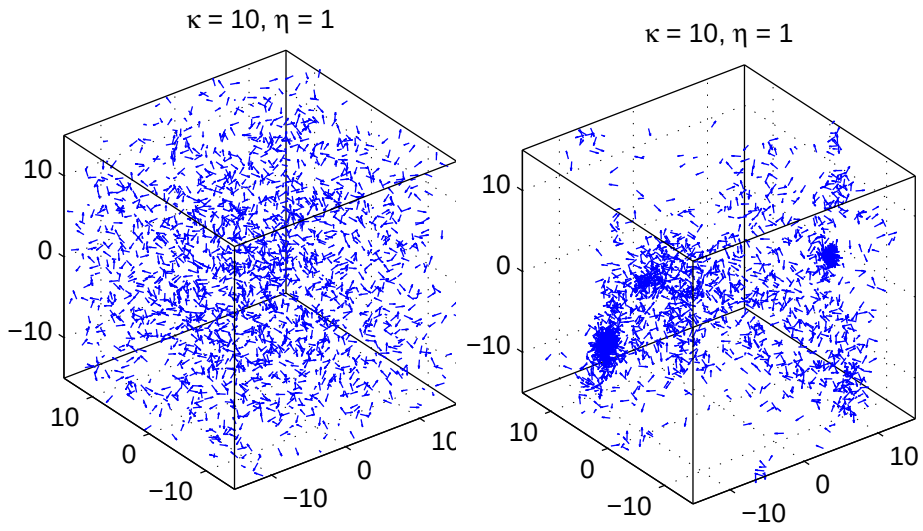

(a) Example of $Q = 1$, homogeneous system

(b) Example of $Q \simeq 100$, clustered system

Figure 2.8: comparison of homogeneou s and clustered systems

2.3.4 Equations of Motion

$$\frac{d\vec{x}}{dt} = |v_0|\vec{e} + \vec{v}_{turb} \tag{2.17}$$

$$\frac{d\vec{e}}{dt} = -\gamma\frac{\partial\vec{U}}{\partial\vec{e}} + \frac{1}{2}(\vec{\omega} \times \vec{e}) + \vec{\eta} \tag{2.18}$$

where v_0 is the constant velocity of each particle; v_{turb} is the velocity of the turbulent flow; $\vec{e}$ is the orientation unit vector; U is the Lebwohl-Lasher potential (2.13); γ is the relaxation constant; $\vec{\omega}$ is the vorticity of the field $\vec{\omega} = \vec{\nabla} \times \vec{v}_{turb}$; $\vec{\eta}$ is the thermal noise factor.

In writing equation (2.18) we took in account the fact that the fluid the particles are swimming in is incompressible and there are no gravitational interactions. We also made use of equation (2.3).

Chapter 3

Implementation

This chapter's aim is to describe the methodologies used to study the system described in the previous chapter. Since simulations were the major part of our work, the chapter will focus on the technicalities.

3.1 The Tools

There was the need to use a few different tools:

Simulation Code We use molecular dynamics simulations with periodic boundary conditions. Simulations, as opposed to the majority of the ones seen in literature, are in three dimensions.

The code is written in C. The reasons we are able to run such performance intensive simulations is because we use a very efficient neighbour list called MLG (Monotonic Logic Grid) to speed up the calculation of mutual interactions between particles. The main idea of the MLG is that neighbours in the simulations are also neighbours in memory making extremely fast to access the neighbour informations. To keep the MLG ordered, it is necessary to sort the grid every timestep. The algorithm we used to sort the particles is the C standard library quicksort.

NOTE: a possible substantial speed up can be reached if the algorithm is parallelised. A way to do so is using Hilbert Curves to span the box space.

To calculate the turbulent velocity field, Kraichnan's method was used. The motion of the particles is implemented by integrating the differential equations: (2.18) and (2.17). Using the Lagrangian lambda method, we impose constraints on the differential equations so that it's easier to integrate them with a velocity Verlet algorithm.

Since the running time was still slow, parallelisation was required to cut the running time even further.

Table 3.1: Example of a simulation input file

Definition	Abbreviation	Value
Number of iterations	iter num	100000
Number of particles in each direction	$N_x N_y N_z$	30 30 30
Size of the simulation box	$L_x L_y L_z$	30 30 30
Interaction range	ϵ	1
Restart simulation switch	starting	-
Particle speed	v_0	0.5
Thermal noise	η	0.01...1
Time step size	Δt	0.1
Relaxation constant	γ	1
Turbulence intensity, number of modes	κ, NF	10^{-4}... 10, 32
Output frequencies	Δpos, ΔS	5000, 500

The simulation code outputs the following data every t_{pos} timesteps:

- spatial configuration of the particles
- particle orientations
- turbulent velocity field at the particles' positions
- angle between the particle orientations and the field vectors
- nematic order parameter

Clustering Script The script is written in C. This routine goes through the particle configurations outputted by the simulation codes and generates a list of neighbours. The cut-off range used is the same that determines the nematic interaction. Once every cluster has a member list, it is possible to calculate quantities such as the number of particles in each cluster or the radius of gyration of each cluster.

Matlab and Minor Scripts Shell scripting was mainly used to automate tedious tasks whereas Matlab was the main tool used for plotting.

In particular, the built-in Voronoi function was very useful to calculate the patch enhancement factors, Q. During the test phase, Matlab was also used to output videos and various three dimensional snapshots of the system.

3.2 Monotonic Logic Grid (MLG)

The monotonic logic grid is one of the main reasons our simulations are so fast. A monotonic logic grid is a data structure where particles are required to obey the following rules:
for a three dimensional particle:

$$x(i,j,k) \leq x(i+1,j,k) \qquad i = 1,..,N_x - 1 \tag{3.1}$$

$$y(i,j,k) \leq y(i,j+1,k) \qquad j = 1,..,N_y - 1 \tag{3.2}$$

$$z(i,j,k) \leq z(i,j,k+1) \qquad k = 1,..,N_z - 1 \tag{3.3}$$

where:
N_x is the number of particles on the x axis
N_y is the number of particles on the y axis
N_z is the number of particles on the z axis

Constraints (3.1), (3.2) and (3.3) make sure that the particles that are neighbours in the simulation are actually neighbours in the memory. The speed access of memory is therefore dramatically increased compared to an unordered structure. This considerably speeds up the code when nematic interaction is calculated. MLGs are a very useful method anywhere there is a neighbouring particle interaction mediated by a cut-off range.

They are widespread in molecular dynamics simulations, but they also find interesting applications in some other less common cases; a good example is the tracking of air traffic[28].

Sorting Algorithms After each timestep calculation it is necessary to sort the particles in the memory along each axis so that the structure remains unchanged. Any sorting algorithms can be easily chosen. Popular choices include: bubblesort, where sorting is done comparing the selected particle with the following particle on that axis; or shellsort, where the comparison is done with the particles offset by half the number of the particles. Bubblesort is efficient in presorted situations whereas shellsort is more effective with random data sets[28]. Shellsort is usually preferred to quicksort when the worst case is relevant.

Stochastic Grid Regularisation Algorithm MLGs are not unique. Very often constructed MLGs do not form an orthogonal grid. For this reason, it is useful complement the MLG with a Stochastic Grid Regularization algorithm(SGR). The SGR works by perturbating the position of a selected particle and using the new configuration to calculate the old MLG. This method is particularly useful when the grid tangles itself and a small perturbation can "straighten" the grid.

A 2D Example The following example is taken from "The Monotonic Lagrangian Grid for Rapid Air-Traffic Evaluation" [28].

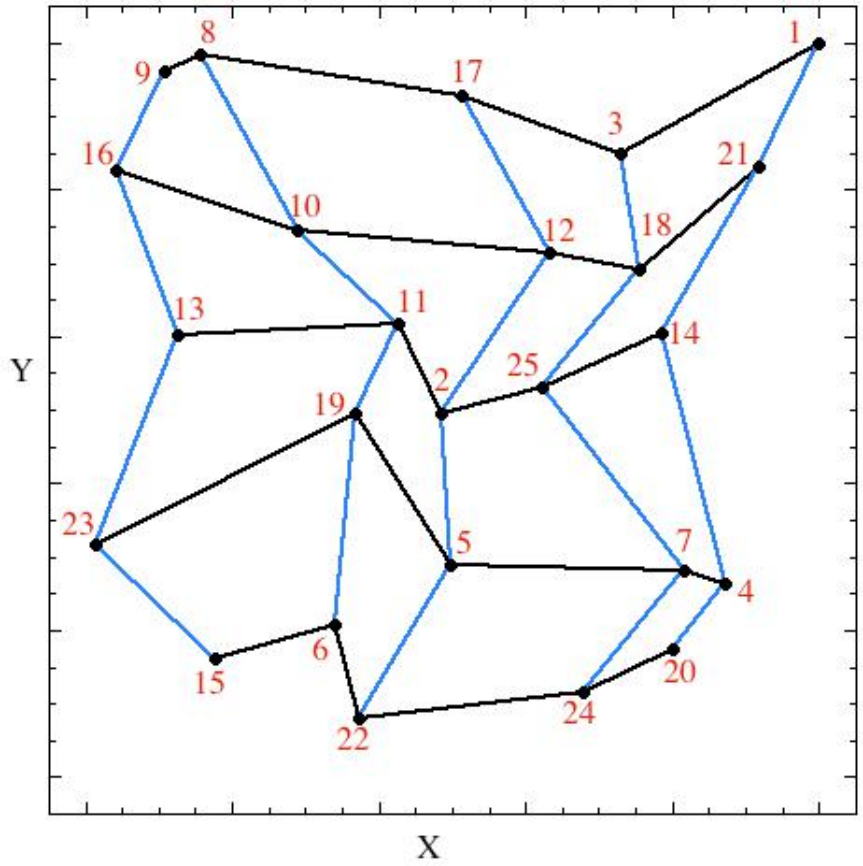

Figure 3.1: "An example of a two-dimensional MLG. The figure shows a 2-D MLG (5x5) containing the x- and ylocations of 25 labeled nodes. The solid black (horizontal) lines show the x-links and the dotted blue (vertical) lines show the y-links. The table shows the regular grid indices of the nodes shown in the figure. That is, node-15 is indexed at i = 1, j =1; node-6 is indexed at i =2, j = 1, etc." (source: "The Monotonic Lagrangian Grid for Rapid Air-Traffic Evaluation")

5	9	8	17	3	1
4	16	10	12	18	21
3	13	11	2	25	14
2	23	19	5	7	4
1	15	6	22	24	20
J/I	1	2	3	4	5

Table 3.2: "shows the regular grid indices of the nodes shown in the figure. That is, node-15 is indexed at i = 1, j =1; node-6 is indexed at i =2, j = 1, etc."

Figure 3.1 shows how the particles are in the simulation whereas the Table 3.2 shows how the particles are indexed in memory. The red numbers in are an arbitrary number used to label particles.

If we were to calculate the neighbour interaction with, say, the particle number 25, knowing that its indices in memory are $I = 4, J = 3$, we would immediately know that the indices $I = 3, 4, 5$ and $J = 2, 3, 4$ are the ones we are interested in for our calculations.

Our implementation We implemented the MLG neighbouring list in C using quicksort from C standard library. We do not use the SGR algorithm. As the neighbour-list is created, the interactions are calculated using the Lebwohl-Lasher interaction (2.13).

3.3 Periodic Boundary Conditions

Periodic boundary conditions are a very important assumption in our model. They model the assumption of studying a small packet of an infinite system where the net flux of matter is zero. Periodic boundary conditions can come in various flavours and they can even be exploited to deform the shape of the simulation box. The most common periodic boundary condition are perhaps the Born-Von Karman, used solid state physics to ensure the periodicity of wavefunctions of a Bravais lattice.

Our system uses a simple very simple implementation: particles that exit a face of the box, must re-enter from the opposite face; the turbulent vector field must be periodic with period equal to the length of the box.

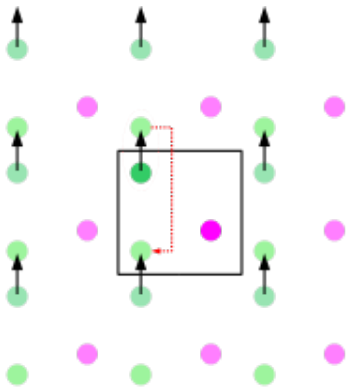

Figure 3.2: A two dimensional example of periodic boundary conditions (source: wikipedia.org)

Configurational PBC Positions of the particles are periodic so that every particle that crosses a boundary re-enters the system from the opposite side of the boundary. The implementation in C can be easily done using the modulus operator related to the box length.

Turbulent Field PBC We also want the turbulent field to respect the PBC to avoid strange boundary artifacts. Periodicity causes our turbulent spectrum to be quantised.

For the periodic boundary conditions to be implemented we want that

$$v_{turb}(-\frac{L}{2}, t) = v_{turb}(+\frac{L}{2}, t) \tag{3.4}$$

this quantises our wave numbers in the following way

$$k_n = \frac{2\pi}{L} \tag{3.5}$$

3.4 Kraichnan's Method

Solving a non-linear partial differential equation is always a daunting task. Solving Navier-Stokes equations (2.2), in three dimensions, might sometimes be impossible. Solutions to two dimensional systems were found, but we are still obliged to use numerical results to study three dimensional systems. As seen in the section regarding turbulence, very often in real systems the type of solutions we are interested in is a particular subset of the very general solution. Therefore solving analytically may not be even necessary.

In our system, we solve all the turbulence related issues with a numerical approximation elaborated by Robert Kraichnan in the 70s[29] The method focuses on a single particle affected by an incompressible, stationary, homogeneous, isotropic, and multivariate normal velocity field. The reason we can simply treat the particles as separated entities is that, in our model, we calculate mutual interaction through the Lebwohl-Lasher potential(2.13).

Kraichnan's method exploits the fact that the turbulent phenomenon can be seen as a superposition of eddies that have a length scale equal to k_n.

(3.6) shows how the turbulent velocity field is calculated at each point in space through a Fourier truncated Series.

$$v_{turb}(\vec{x}, t) = \sum_{n=1}^{N_F} (\hat{c}_{1,n} cos\Omega_n + \hat{c}_{2,n} \sin\Omega_n)|\vec{c}_n| \tag{3.6}$$

where:
N_F is the number of modes we compute; $\hat{c}_{1,n} = \vec{a}_n \times \vec{k}_n$ and $\hat{c}_{2,n} = \vec{b}_n \times \vec{k}_n$; $\vec{a}_n$ and $\vec{b}_n$ are random unit vectors; and $\Omega_n = \Omega_n(t, \vec{x}) = (\vec{k}_n \cdot \vec{x} + \omega t)$.

The field intensity can be easily written as sum of sines and cosines. Numerical precision is proportional to the number of modes that we decide to sum. We always used $N_F = 30$, but in literature it is often equal to a power of 2, for example $N_F = 32$ or $N_F = 64$ [30]. For more details about the number of modes necessary, we recommend Fung's work[31].

3.5 Velocity Verlet Integration

Computational models always need to deal with the fact that the precision of a computer is discrete. Numerical analysis is the branch of mathematics that studies the discrete algorithms used to solve a variety of problems such as integrating differential equations.

When integrating numerically a differential equation, there are three important factors to take in account when choosing the correct algorithm:

- convergence: does the numerical solution converge to the analytical solution we are looking for?
- order: what is the error committed by one iteration of the algorithm?
- stability: is the solution stable or does it oscillate?

When integrating equations of motion such as (2.17) and (2.18), the most intuitive, yet somewhat imprecise way to integrate would be using an Euler algorithm.

The Euler algorithm:

$$x(t_0 + h) = x(t_0) + hx'(t_0) + \frac{1}{2}h^2x''(t_0) + O(h^3) \tag{3.7}$$

This algorithm is only of the first order and since we also need to integrate the variation of velocity (2.18), we are looking for a more sophisticated algorithm.

The algorithm we decided to use gets its name from Loup Verlet, the French Physicist that popularised its use in molecular dynamics; the algorithm is called velocity Verlet and operates in the following way:

1. $\vec{x}(t + \Delta t) = \vec{x}(t) + \vec{v}(t)\,\Delta t + \frac{1}{2}\,\vec{a}(t)\,\Delta t^2$
2. $\vec{v}(t + \Delta t) = \vec{v}(t) + \frac{1}{2}\,\left(\vec{a}(t) + \vec{a}(t + \Delta t)\right)\Delta t$

where $\vec{a}(t)$ is found deriving the interaction potential (see (2.18)); $\vec{x}(t)$ is the position; $\vec{v}(t)$ is the direction; and Δt is the discrete timestep used to integrate the equation.

The algorithm integrates both velocity and positions at the same timestep.

Velocity Verlet is a second order algorithm and its computable as Euler, without additional cost. It has a good numerical stability and preserves some important physical characteristics of the phase space. This explains its wide usage in molecular dynamics.

We use this algorithm in conjunction with the lambda method to further simplify the second step of the integration

3.6 Lambda Method and Viscosity

In our model, the viscosity of the fluid has not yet been talked about. Viscosity is both important because we are studying low Reynolds number fluids, and, by definition, this means that viscous forces are far stronger that inertial ones. It is also known that viscosity is key in the dissipative nature of turbulence: eddies break into smaller scaled versions of themselves, until the fluid viscosity is able to dissipate the energy completely.

In our system viscosity sets the non conservation of energy which avoids the system from having unwanted behaviour.

Viscosity is implemented by constraining the direction vector on a sphere of unitary radius. The constraint also helps to solve the differential equations with the Lagrangian multiplier method. This is how the differential equation for the direction of the particle(2.18) can be written:

$$\dot{\vec{e}} = \vec{T}^{\perp} + \lambda\vec{e} + \frac{1}{2}(\vec{\omega} \times \vec{e}) \tag{3.8}$$

where $T^{\perp}$ is intended as the perpendicular component of torque particle; λ is the coefficient that comes from the Lagrange method; and for the other definitions look at Equation (2.18).

$T^{\perp}$ can also be written in the following way:

$$T^{\perp} = \vec{T} - \vec{T}^{\parallel} = \vec{T} - (\vec{T} \cdot \vec{e})\vec{e} \tag{3.9}$$

where $T^{\parallel}$ the parallel component of the torque on the particle.

The velocity Verlet equations then becomes:

$$\vec{r}(t + \Delta t) = \vec{r}(t) + (|v_0|\vec{e}(t) + \vec{u}(r, t))\Delta t \tag{3.10}$$

where $\vec{u}(r, t)$ is the turbulent field intensity at the current point and timestep.

$$\vec{e}(t + \Delta t) = \vec{e}(t) + \Delta t\vec{T}^{\perp} + \Delta t(\lambda\vec{e}(t) + \frac{1}{2}(\vec{\omega} \times \vec{e})) \tag{3.11}$$

where we used the (3.8) to write the velocity verlet equation. We also keep in mind that

$$\Delta t\vec{T}^{\perp} = (-\gamma\frac{\partial U}{\partial\vec{e}} + \vec{\eta})_{\perp}\Delta t = (2\gamma\frac{1}{n_n}\sum_j(\vec{e} \cdot \vec{e}_j)\vec{e}_j + \eta\vec{\epsilon})_{\perp}\Delta t \tag{3.12}$$

Remembering the definitions given for (2.18).

The equation (3.11) shows the exact integration used in the simulations.

Chapter 4

Results

In this chapter we show the main plots concerning our work. Clustering is studied with a three pronged approach: the first is the most conventional, used also by Stocker which use the patch enhancement factor Q. The second takes in account the number of particles in the biggest cluster, the last uses the radius of gyration of the largest cluster in the system. Alignment of the system is studied using the previously defined nematic order parameter.

4.1 Q(f) Plots

The Q factor is calculated according to the previously given definition (see Equation(2.15)). The densities are calculated by constructing Voronoi cells around each particle and calculating the volume of each cell. Particles were subsequently ordered from denser to sparser and the f fraction of most dense particles were used to calculate our $Q(f)$ factor.

To choose the the optimal f, three dimensional snapshots of the most clustered systems were analysed at various fractions. The cherry picked value wants to highlight the difference between the clustered and unclustered particles without showing too much visual noise caused by the non clustered particles.

The optimal value was established to be $f = 0.05$ half of the one used by Stocker.

Figure 4.2 with $Q(f = 0.1)$ was nonetheless included to give a term of comparison with the peer reviewed paper.

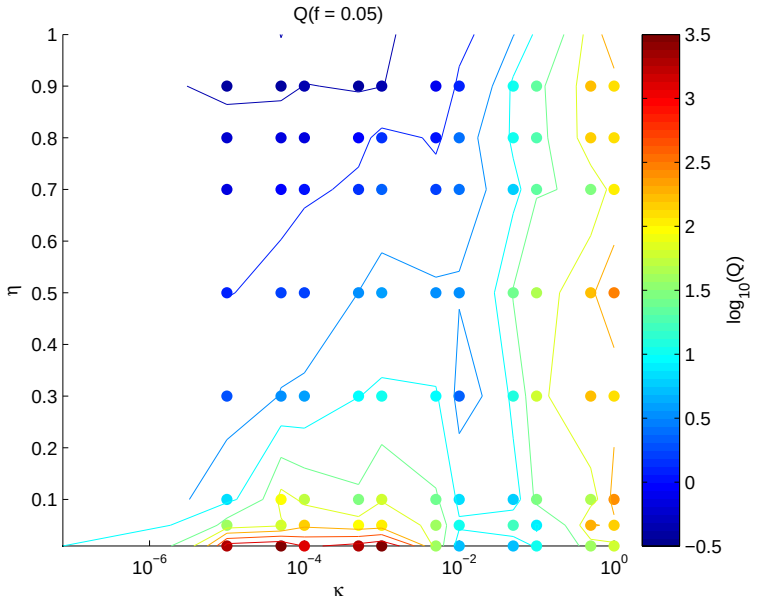

Figure 4.1: plot of the patch enhancement factor $Q(f = 0.05)$ varying the parameters kappa, turbulent field intensity; and eta, thermal noise

Figure 4.1 is the central result of our research. There we show the dependence of $Q(f)$ on the turbulent field intensity κ (on the horizontal axis) and on the intensity of the thermal noise η (on the vertical axis). We find that the clustering can reach values up to $10^{3.5}$ times the average density of particles. What is most interesting is that a high degree of clustering is found in the systems with large κ, that is strong turbulence, regardless of the noise. So whereas at weak turbulent intensities we see that the noise is able to disrupt clustering (top left corner of the plot), at stronger turbulence, thermal noise is more or less ignored.

Since active particles are usually able to vary their speed, they have a degree of control on the mutual interactions which, in turn, affects the turbulence in the system. Our result suggests that particles could induce clustering in a thermally noisy environment simply by adjusting their swimming speed.

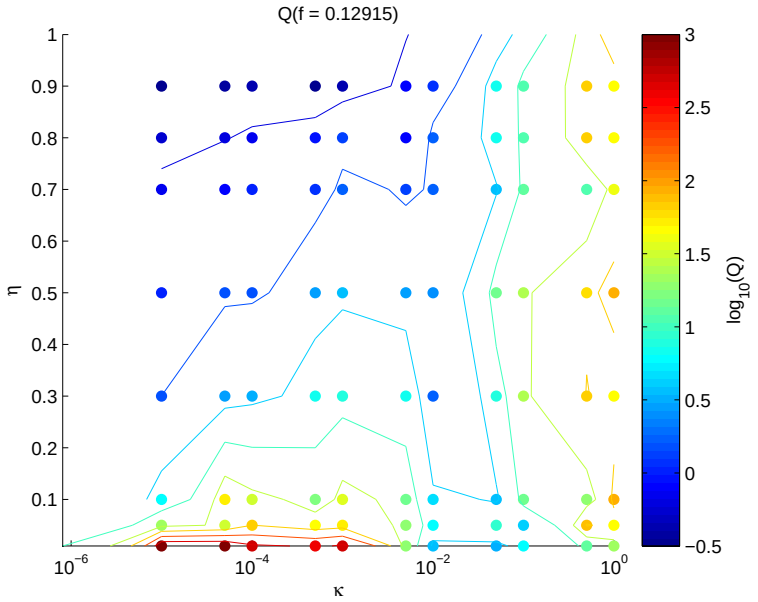

Figure 4.2: plot of the patch enhancement factor $Q(f \simeq 0.1)$ varying the parameters kappa, turbulent field intensity; and eta, thermal noise; this plot is just a term of comparison with Stocker's

4.2 Cluster Radius

The following study of the clusters uses a different methodology from one used in the calculation of Q systems. The previous analysis constructed Voronoi cells for each particle and, taking the inverse of the volume of each cell, computed and assigned a density value for each particle. In this study, we used a C routine to run through all the spatial configurations of particles and check whether they are within a cut-off range. The cut-off range is the same range used for the nematic interaction between each particle.

Once it is established that the particles are part of the same cluster, the script can characterise the cluster in many more ways calculating some interesting quantities.

In this case we computed the gyradius(or radius of gyration) of each cluster (see eq. (2.16)) and then we selected the maximum one for every simulation.

The configurations used for the calculation are, of course, the same used for the study with the Voronoi cells,

Figure 4.3 shows the variation of maximum gyradius in the system, $\max(R_g)$, as a function of the turbulent field intensity κ (on the horizontal axis) and the intensity of the thermal noise η (on the vertical axis). We remind the reader that the box has a length of $L = 30$ and $\max(R_g) = 10^{1.5} \simeq 31.63$, the maximum value, is close to the one dimensional length of the box, but in principle it could even reach the length of the diagonal of the box since we are in three dimensions.

Low κ result in a system that is mainly driven by the thermal noise: the higher the η, the smaller the radius.

High κ systems seem to ignore completely the thermal noise when it comes to clustering radius.

The results are coherent with the ones found in figure 4.1

This is very sensible since $\rho \propto \frac{1}{r^3}$.

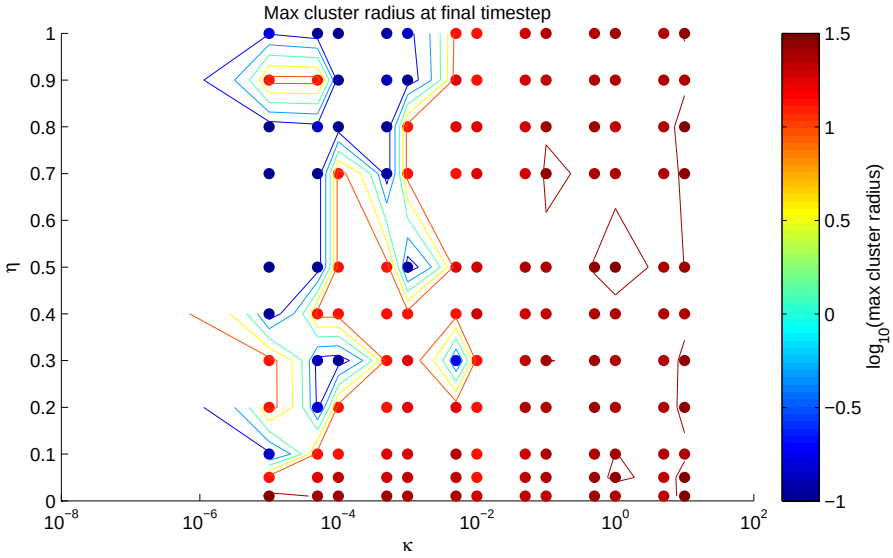

Figure 4.3: maximum radius of gyration varying the parameters kappa, turbulent field intensity; and eta, thermal noise

In nature, the radius of the cluster could affect the behaviour of the active swimmers in many ways. If particles are able to vary the radius of the cluster, it means they are able to distribute in space in a favourable way so that they can either reach food or flee from toxins. Depending on the specific swimmer, various understandings on the behavioural traits can be carried on.

4.3 Cluster Crowdedness

This study uses the same C script used in the gyradius calculation. Once all the spatial configurations of each particle are analysed to give an accurate list of the clustered particles, the number of particles in every cluster is calculated.

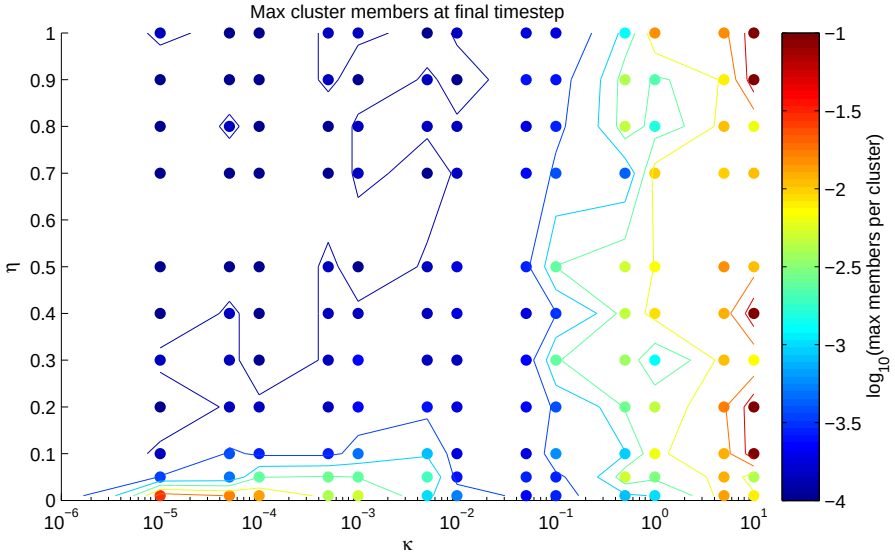

Figure 4.4: maximum number of particle in the largest cluster varying the parameters kappa, turbulent field intensity; and eta, thermal noise

Figure 4.4 shows the maximum number of cluster members in each system as a function of the turbulent field intensity (on the horizontal axis) and the thermal noise (on the vertical axis).

The plot, even though very noisy, shows something familiar: small turbulence causes the system to be governed by the thermal noise, which tends to let particles gather in very small-populated clusters; higher turbulence enables the system to gather more particles in the same cluster; low noise allows clustering to be achieved without too much turbulence.

Q comparison We clearly see that the result is coherent with figure 4.1. Once again, this makes sense because the $\rho \propto N_{particles}$

As opposed to the other plots, this one shows a high degree of noise. This is caused by the fact that only one simulation was used to calculate the number of particles in the most crowded cluster. It is possible to reduce the noise running a set of simulations with the same parameters but different random initial seed. Another alternative is analysing the time evolution of the values and calculate a mean.

4.4 Nematic Order Parameter plot

The nematic order parameter is a way to know if the system aligns to a given axis. Details on the calculation can be found in the homonimous section.

Figure 4.5 shows the nematic order parameter in each system as a function of the turbulent field intensity (on the horizontal axis) and the thermal noise (on the vertical axis). Contour lines help to highlight different areas of the parameter space which could interest us. We can clearly see that both κ and η have a disrupting effect on the nematic symmetry of the system, that is, they both restore the broken symmetry of the system.

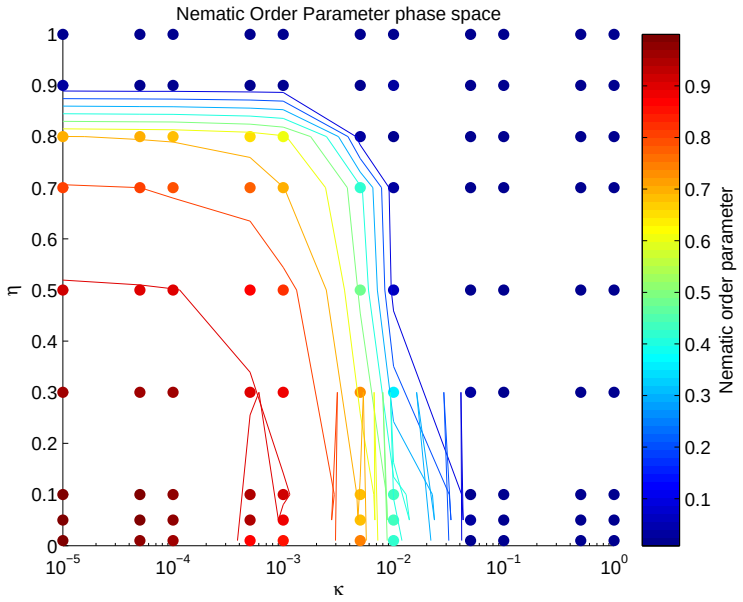

Figure 4.5: contour lines of the nematic order parameter plot varying the parameters kappa, turbulent field intensity; and eta, thermal noise

Correspondence Principle It is noteworthy to look at figure 4.6 and the first column of dots on the y axis in figure 4.5. Due to the logarithmic scale, that column represents the system with turbulent interaction switched off. We can see that there is a really close a nematic-isotropic phase transition curve we would find on a textbook (and in the Mazza-Breier model). The curve starts with a system almost entirely aligned in a direction, that is nematic order parameter, $S \simeq 1$, and as the thermal noise increases (temperature) there is a continue transition towards a completely isotropic phase, $S = 0$.

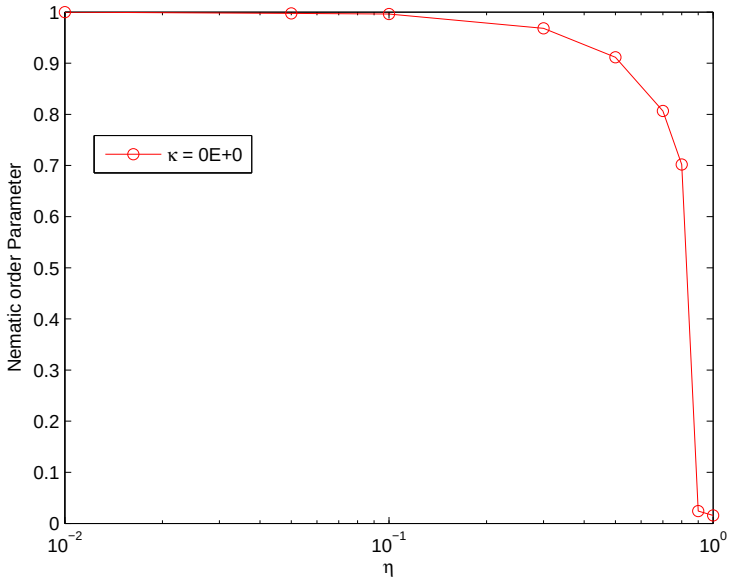

Figure 4.6: nematic order parameter in laminar flow

Chapter 5

Conclusions

To recap, active particles that swim in low Reynolds numbers fluids interact with one another very often generating turbulent effects in the fluid. Our main result is that nematic particles are able to form larger clusters thanks to turbulence; high turbulence helps the particles to ignore the cluster-disrupting effect of thermal noise, as a consequence local density values is allowed to reach values up three orders of magnitude larger than the homogeneous counterpart.

A second result is that, when clustered, the particles tend to align isotropically. Therefore turbulence (or the effects of it, so clustering) cause the isotropic symmetry to be recovered just as temperature would do.

The main result is very interesting because nature exhibits many cases where clustering creates favourable conditions for active swimmers; for example, spermatozoa of the wood mouse swim faster in a clustered configuration than as isolated cells[18].

Chapter 6

Outlook

In research, very often a result leads to many, more questions. We have found clustering in our system, we found when the system prefers such configurations, but there are many open questions.

Faster Simulations The running time of the simulations ranges from a few hours to several days. This time is what is needed to plot a single point in graphs such as figure 4.5 or figure 4.1. Speeding the code would not only speed up the data gathering, but also help us explore new variations of the system that were previously computationally impractical.
The actual state of parallelisation uses openMP for the main loops. The speed up was very impressive, but the running time is still lengthy. An obvious solution to this problem is port the performance critical parts of the code to a natively parallel language (using CUDA C or Julia) and/or, since the code is intended to run on CPU clusters, even think of a good MPI implementation.

Time Analysis of the Clustering At the moment we study clusters only at the utmost timestep. Studying the time evolution of the clusters can help us gain insight on the time scales of these clustering effects and gives more statistical data

Variable Density All the simulations were run with a concentration $C = \frac{N_{particles}}{L_{box}^3} = 1$. Varying the densities as a parameter could help shed further light on systems such as the ones encountered in nature.

Bigger Boxes Turbulent phenomena are highly affected by the boundaries. Larger boxes result in reducing the boundary effects thus giving us a more precise representation of our system.

Different Particles It would be very interesting to study variable particle velocities for at least two reasons: first, it models genetic variance; second, it models an ability that most of the living active particles have: varying the cruising speed to suit their needs. Another interesting improvement would be modelling the size of the particles through a hard core potential. Sizes could even be randomly generated.

More Phase Transitions The Mazza-Breier model, shows that nematic active particles exhibit other peculiar phases like the Chiral, the Smectic, and even coexistence between different phases. How does the turbulence affect these phases? Is there the chance of observing coexistence?

Generalising the Particle Shape Our model studies nematic particles whereas there are many models that study the spherical counterparts. Finding the former as a limit of the latter (or vice versa) would help understanding the clustering in specific bacteria with different, regular shapes.

Chapter 7

Acknowledgements

First of all, I want to thank my parents which always put my needs before theirs, I also want to thank my cousin Treshan who is, to this day, an inspiration for me. I really thank the people who introduced me to the world of research: Rebekka Breier who helped me even during pregnancy and maternal leave, and Marco Mazza who has always a wise answer to my questions. Special thanks go to Hannes Hornischer and Giulio G. Crespi who helped me choose this work as my thesis. I also thank the people who made this work possible: Professor Alberto Vailati who gave me the permission to discuss my thesis in Milan and a few, but very useful tips; and Professor Nicola Piovella, the manager of the Erasmus programme at our department.
A quick thank you to all the members Non-Equilibrium Statistical Mechanics (NESMians) at the Max Planck Institut für Dynamik und Selbstorganisation in Göttingen, Germany that made the work lighter and playful (in alphabetic order): Qiong Bai, Peleg Bar Sapir, Matthias Hummel, Victor Meiwes-Turrion, Lee Kuang Wu (Jeff), Henning Zwirnmann. Double thanks to Henning whose kindness I will never forget.

Bibliography

[1] Marchetti M C Baskaran A. "Statistical mechanics and hydrodynamics of bacterial suspensions". In: *PNAS* (2009).

[2] Ciccotti G Herminghaus S Mazza M G Breier R E Selinger R L B. "Spontaneous chiral symmetry breaking in model bacterial suspensions". In: *cond mat soft* (2014).

[3] Frank K de Boisfleury-Chevance A Gruler H Schienbein M. "Migrating Cells: Living Liquid Crystals". In: *Mol. Cryst. Liq. Cryst.* (1995).

[4] Schrank-Kaufmann S Kaufmann D Gruler H Kemkemer R Teichgräber V. "Nematic order-disorder state transition in a liquid crystal analogue formed by oriented and migrating amoeboid cells". In: *PNAS* (2000).

[5] Ben-Jacob E Cohen I Shochet O Vicsek T Czirok A. "Novel type of phase transition in a system of self-driven particles". In: *Phys. Rev. Lett.* (1995).

[6] Delcourt J Poncin P Becco C Vandewalle N. "Experimental evidences of a structural and dynamical transition in fish school". In: *Physica A: Statistical Mechanics and its Applications* (2006).

[7] Couzin I D Hale J J Despland E Miller E R Simpson S J Buhl J Sumpter D J T. "From Disorder to Order in Marching Locusts". In: *Science* (2006).

[8] Powers T R Lauga E. "The hydrodynamics of swimming microorganisms". In: *Reports on Pogress in Phyysics* (2009).

[9] In:

[10] Wilkening K Anderson K R Mendelson N H Bourque A and Watkins J C. "Organized cell swimming motions in Bacillus subtilis colonies: patterns of short-lived whirls and jets". In: *J. Bacteriol.* (1999).

[11] Kessler J. "Dynamics of swimming bacteria at low and high volume fraction". In: *Proc. Int. Conf. on Differential Equations (Berlin, Germany, 17 August 1999).*

[12] Wu X L and Libchaber A. "Wu X L and Libchaber A". In: *Phys. Rev. Lett.* (2000).

[13] Chatkaew S Goldstein R E Dombrowski C Cisneros L and Kessler J O. "Self-concentration and large-scale coherence in bacterial dynamics". In: *Phys.Rev.Lett.* (2004).

[14] Dombrowski C Goldstein R E Cisneros L H Cortez R and Kessler J O. "Fluid dynamics of self-propelled micro-organisms, from individuals to concentrated populations". In: *Exp. Fluids* (2007).

[15] Kessler J O Sokolov A Aranson I S and Goldstein R E. “Concentration dependence of the collective dynamics of swimming bacteria”. In: *Phys. Rev. Lett.* (2007).

[16] Wolgemuth C W. “Collective swimming and the dynamics of bacterial turbulence”. In: *Biophys. J.* (2008).

[17] Pacey A A Suarez S S. “Sperm transport in the female reproductive tract”. In: *Human Reprod.* (2006).

[18] Jenkins N Moore H Dvorakova K and Breed W. “Exceptional sperm co-operation in the wood mouse”. In: *Nature* (2002).

[19] Moore H D M and Taggart D A. “Sperm pairing in the opossum increases the efciency of sperm movement in a viscous environment”. In: *Biol. Reprod.* (1995).

[20] Hayashi F. “Sperm co-operation in the Fishy Parachauliodes japonicus”. In: *Funct. Ecol.* (1998).

[21] Barry M Lillo F D Boffetta G Cencini M Stocker R Durham W M Climent E. “Turbulence drives microscale patches of motile phytoplankton”. In: *Nat Commun* (2013).

[22] *Fluid Mechanics*. Elsevier Academic Press, 2012.

[23] Taylor G I. “Diffusion by continuous movements”. In: *Proceedings of the London Mathematical Society* (1921).

[24] Taylor G I. “Eddy motion in the atmosphere”. In: *Philosophical transactions of the Royal Society of London* (1915).

[25] *Weather Pretiction by Numerical Process*. Cambridge University Press, 1922.

[26] Kolmogorov A N. “The local structure of turbulence in incompressible viscous fluid for very large Reynolds numbers”. In: *Doklady Akademii Nauk SSSR* (1941b).

[27] Kolmogorov A N. “Dissipation of energy in locally isotropic turbulence”. In: *Doklady Akademii Nauk SSSR* (1941a).

[28] Oran E Alexandrov N Boris J Kaplan C Dahm J. “The Monotonic Lagrangian Grid for Rapid Air-Traffic Evaluation”. In: *10th AIAA Aviation Technology, Integration, and Operations (ATIO) Conference*.

[29] Kraichnan R H. “Diffusion by a Random Veloity Field”. In: *The Physics of Fluids* (1970).

[30] Visser A W Botte V Mariani P MacKenzie B R. “Individual-based simulations of larval fish feeding in turbulent environments”. In: *Mar Ecol Prog Ser* (2007).

[31] Malik N A Perkins R J Fung J C H Hunt J C R. “Kinematic simulation of homogeneous turbulence by unsteady random Fourier modes”. In: *J. Fluid Mech.* (1992).